Full Model-Based Analysis of QUASAR Arterial Spin Labelling

M. A. Chappell[1,2], E. T. Petersen[3], M. W. Woolrich[2], X. Golay[4], and S. J. Payne[1]
[1]Institute of Biomedical Engineering, University of Oxford, Oxford, United Kingdom, [2]FMRIB Centre, University of Oxford, Oxford, United Kingdom, [3]Clinical Imaging Research Center, NUS-A*STAR, Singapore, [4]Institute of Neurology, University College, London, United Kingdom

Introduction: QUASAR is a multi-slice multi-TI pulsed arterial spin labelling (ASL) sequence that employs a mixture of flow suppressed and non-suppressed images to estimate separately the time course of tissue and arterial labelled blood within the brain [1]. The choice of flow suppression directions means that theoretically all that is required is simple addition and subtraction of the data to produce tissue and arterial ASL data. This can then be used within a 'model-free' analysis approach that attempts to estimate CBF from the deconvolution of an arterial input function (estimated from the arterial data) with the tissue curve [1]. It has been shown recently that it is feasible to use a model-based method to separate tissue and arterial signal contributions in ASL data acquired without flow suppression [2]. The same principle could be applied to QUASAR data with the advantage that the combination of suppressed and non-suppressed data should improve the separation. Comparisons between model-based and model-free methods to-date have not sought to make full use of the information within QUASAR data using a model-based framework. This work aimed to rectify this by proposing a novel two component model-based analysis for QUASAR ASL.

Methods: The model-based analysis involved two stages: firstly, prior to tag-control subtraction, a saturation recovery curve model was fit to the data to estimate M_{0t} (the equilibrium magnetization of the tissue), T_{1t} and a correction factor to account for variations in the true flip angle from that specified (this exploits the presence of the low flip angle measurement in the QUASAR sequence). These values were then employed as the prior mean values for these parameters in the subsequent analysis stage. The second stage was the fitting of a two-component kinetic curve model to the data containing the signal that is assumed to arise from both labelled blood undergoing exchange within the tissue space and that remaining within the arterial vasculature. To account for the various cycles of flow suppression it was assumed that: in the absence of flow suppression the signal contained both tissue and arterial components; in the presence of flow suppression the tissue component would be unaffected, but the arterial component would be reduced depending upon the correspondence between the blood flow direction and that of the suppression. Thus the dominant arterial blood flow direction was a further parameter of the model that was inferred from the data. It has already been shown that the effects of the dispersion of labelled blood during transit through the vasculature are significant in ASL, thus a number of kinetic curve models were considered. In each case the shape of the arterial component was specified and this same form was assumed for the arterial input function for the tissue component, parameters of the arterial shape (for example, bolus duration and 'dispersion' parameters) were shared by both components. The arterial shapes considered were A) the **standard** model of [3] that assumes no dispersion, B) the Gamma-variate function (**GVF**) (characterised by a time-to-peak, *p*, and sharpness, *s*) widely used in Dynamic Susceptibility Contrast MRI and previously applied to QUASAR ASL [4], C) the vascular transport model (VTM) of [5] with a Gaussian dispersion function (**gauss**), D) the VTM with a gamma dispersion function (**gamma**). Model fitting was performed using a probabilistic method that has previously been applied to ASL data [4] that allows appropriate prior information about model parameters to be included. Data were also analysed using the model-free method [1] and more conventional model-based analysis, where the tissue only data was extracted in the same way as for the model-free method and then fit with a tissue only component model (using the same probabilistic method).

Data were analysed from 7 subjects each having been scanned 4 times over two sessions (as part of the QUASAR reproducibility study [6]). Scan parameters: TR/TE/ΔTI/TI1=4000/23/300/40 ms, 13 TIs (40-3640 ms), 64x64 matrix, 7 slices, slice thickness 6 mm with 2 mm gap, FOV 240x240 mm, flip-angle=35/11.7°, SENSE=2.5. 6 repetitions containing 3 non flow suppressed pairs (1 with low flip angle) and 4 pairs with flow suppression (V_{enc} 4 cm/s), a total of 84 measurements with duration 5 mins 52 s.

Comparison of the analyses was performed using the mean estimated CBF values within a grey matter (GM) mask defined by automated segmentation of the T1 weighted structural image and transformed into the same space as the ASL images using a rigid body transformation. Estimated CBF images were also transformed into MNI152 standard space using a 12 degree-of-freedom rigid transformation. To examine the spatial variability in estimated CBF when dispersion was included within the model-based analysis, the standard space CBF images were scaled by the mean GM CBF value to give a relative CBF (relCBF) image that was independent of the global changes in estimated CBF introduced by the different models. The dispersion model results were compared to the standard model (no dispersion) by taking the voxelwise mean of the difference in relCBF.

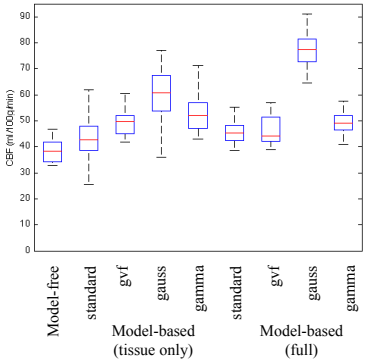

Fig. 2 Mean GM CBF across datasets for the different analysis methods

Results: Fig. 1 shows example CBF and aBV images from the model-free and model-based (on full data) analyses with Fig. 2 showing the mean GM CBF for all the analyses across all the datasets. Estimated aBV appeared to be relatively low for the Gaussian VTM dispersion model implying poor separation of arterial and tissue components and thus resulting in higher CBF estimates, particularly for analysis of the full data. Fig. 3 shows the difference in estimated relCBF between the three dispersion models and the non-dispersed case (shown as ΔrelCBF/relCBF). For all the dispersion models the main regions of difference in the estimated CBF were in watershed regions and white matter. For a GVF arterial shape the white matter CBF was smaller relative to mean GM CBF than without dispersion, whereas with the Gaussian VTM the opposite was true.

Discussion: The analysis method proposed here seeks to fully exploit the information present in QUASAR data rather than simply attempting model fitting on the tissue only data. The results here suggest this does influence the estimated CBF, possibly due to incomplete separation of tissue and arterial time courses when simple subtraction is used. The method proposed here should provide a more appropriate comparison to the model-free approach for QUASAR data in future comparisons of these approaches. Since QUASAR data contains information on arterial and tissue signal components it is very suitable for the examination of different dispersion models. The preliminary investigations carried out here imply substantial spatial differences in estimated CBF arise from the choice of dispersion model. Future investigation should examine the 'goodness-of-fit' of the different models particularly in the arterial signal, since the effects of dispersion cannot be readily separated from restricted exchange in the tissue signal.

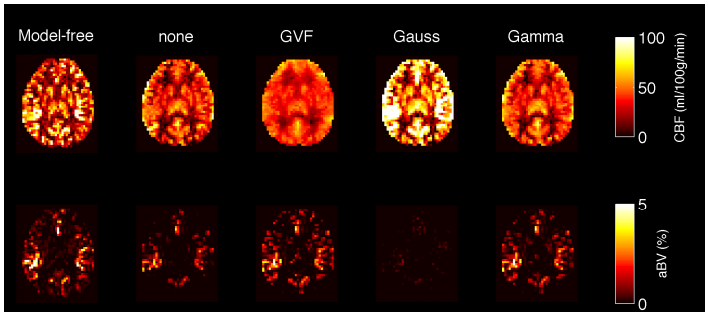

Fig. 1 Estimated CBF and aBV images from the model-free and full model-based analyses from a single acquisition (standard model with no dispersion).

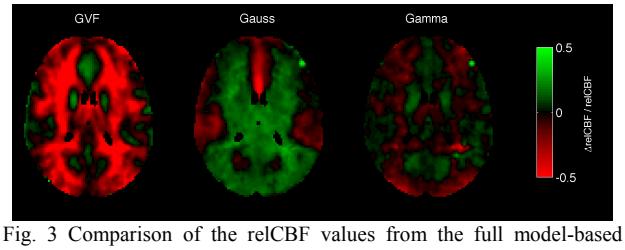

Fig. 3 Comparison of the relCBF values from the full model-based analysis incorporating dispersion to the standard model (no dispersion).

References:
1. Petersen et al., MRM 55:219-232, 2005.
2. Chappell et al., MRM 63:1357-1365, 2010.
3. Buxton et al., MRM 40:383-396, 1998.
4. Hrabe et al., MRM 167:49-55 ,2004.
5. Chappell et al., IEEE Trans. Sig. Proc. 57:223-236, 2009.
6. Petersen et al., NeuroImage 49:104-113, 2010.